ROCK Mediates Phorbol Ester-induced Apoptosis in Prostate Cancer Cells via p21^{Cip1} Up-regulation and JNK*$^{[S]}$

Liqing Xiao[‡1], **Masumi Eto**[§], and **Marcelo G. Kazanietz**[‡2]

From the ‡Department of Pharmacology, University of Pennsylvania School of Medicine, Philadelphia, Pennsylvania 19104-6160 and the §Department of Molecular Physiology and Biophysics, Thomas Jefferson University, Philadelphia, Pennsylvania 19107

It is established that androgen-dependent prostate cancer cells undergo apoptosis upon treatment with phorbol esters and related analogs, an effect primarily mediated by PKCδ. Treatment of LNCaP prostate cancer cells with phorbol 12-myristate 13-acetate (PMA) causes a strong and sustained activation of RhoA and its downstream effector ROCK (Rho kinase) as well as the formation of stress fibers. These effects are impaired in cells subjected to PKCδ RNA interference depletion. Functional studies revealed that expression of a dominant negative RhoA mutant or treatment with the ROCK inhibitor Y-27632 inhibits the apoptotic effect of PMA in LNCaP cells. Remarkably, the cytoskeleton inhibitors cytochalasin B and blebbistatin blocked not only PMA-induced apoptosis but also the activation of JNK, a mediator of the cell death effect by the phorbol ester. In addition, we found that up-regulation of the cell cycle inhibitor p21^{Cip1} is required for PMA-induced apoptosis and that inhibitors of ROCK or the cytoskeleton organization prevent p21^{Cip1} induction. Real time PCR analysis and reporter gene assay revealed that PMA induces p21^{Cip1} transcriptionally in a ROCK- and cytoskeleton-dependent manner. p21^{Cip1} promoter analysis revealed that PMA induction is dependent on Sp1 elements in the p21^{Cip1} promoter but independent of p53. Taken together, our studies implicate ROCK-mediated up-regulation of p21^{Cip1} and the cytoskeleton in PKCδ-dependent apoptosis in prostate cancer cells.

The protein kinase C (PKC)[3] family of serine-threonine kinases has been widely implicated in the control of mitogenesis, cell survival, apoptosis, and differentiation. Based on their different structural organization and biochemical regulation by lipids and calcium, PKCs have been classified into three groups: classical or conventional (PKCα, -β, and -γ), novel (PKCδ, -ε, -η, and -θ), and atypical PKCs (PKCζ and -λ). Both conventional PKCs and novel PKCs are the target for the phorbol esters, natural products that mimic the action of the lipid second messenger diacylglycerol (1, 2). Despite their well characterized tumor promoter activity, phorbol esters cause dissimilar effects, since they can either stimulate proliferation and survival or, conversely, induce cell growth arrest or trigger apoptotic cell death, depending on the cell type (2, 3). Such diversity relates primarily to the differential expression of PKC isozymes according to cell type as well as to the great divergence in the signaling events modulated by individual PKCs. One of the key PKC isozymes implicated in negative growth regulation is PKCδ. Work from several laboratories, including ours, established that PKCδ modulates the transition from G_1 to S phase of the cell cycle by controlling the phosphorylation status of retinoblastoma (4–6). In bronchoalveolar adenocarcinoma cells, activation of PKCδ in early G_1 leads to G_1/S arrest through the induction of p21^{Cip1} at a transcriptional level (4).

Among the few cell types that undergo apoptosis in response to phorbol esters, androgen-responsive prostate cancer cells have been one of the best characterized models. Phorbol 12-myristate 13-acetate (PMA) triggers an apoptotic response in androgen-dependent prostate cancer cells, including LNCaP, C4-2, and CWR22-Rv1 cells (7–9). The mechanisms underlying the cell death effect of phorbol esters in prostate cancer cells are only partially understood, but they seem to involve the p21^{Cip1}/retinoblastoma pathway (10). Our previous studies established that this effect is primarily mediated by PKCδ, and subsequent analysis revealed that this kinase promotes the activation of the extrinsic apoptotic cascade via an autocrine mechanism. PMA promotes the secretion of death factors from LNCaP cells via PKCδ, including TNFα and TRAIL, and the released factors promote cell death via activation of JNK and p38 MAPK cascades (11, 12).

The mammalian Rho GTPases comprise >20 proteins, among which Rac1, Cdc42, and RhoA have been the most widely studied. These small G-proteins have been established as important mediators of receptor signaling and control a variety of cellular functions related to cell division and morphology. Upon receptor activation, Rho GTPases dissociate from Rho guanine nucleotide dissociation inhibitors (Rho-GDIs), allowing Rho guanine nucleotide exchange factors (Rho-GEFs) to switch GDP by GTP and Rho activation (13). Members of the Rho family were originally established as key regulators of cytoskeletal organization in response to extracellular growth factors. Studies over the past few years have revealed that Rho GTPases also play crucial roles in diverse cellular events, such as transcriptional regulation, cell cycle control, endocytosis,

---

$^{[S]}$ The on-line version of this article (available at http://www.jbc.org) contains supplemental Figs. S1 and S2.

[1] Supported by a postdoctoral fellowship from the Department of Defense.

[2] To whom correspondence should be addressed: Dept. of Pharmacology, University of Pennsylvania School of Medicine, 1256 Biomedical Research Bldg. II/III, 421 Curie Blvd., Philadelphia, PA 19104-6160. Tel.: 215-850-6187; Fax: 215-746-8941; E-mail: marcelog@upenn.edu.

[3] The abbreviations used are: PKC, protein kinase C; AdV, adenovirus; GFP, green fluorescence protein; JNK, c-Jun NH$_2$-terminal kinase; MAPK, mitogen-activated protein kinase; PMA, phorbol 12-myristate 13-acetate; RNAi, RNA interference; TNF, tumor necrosis factor; GDI, guanine nucleotide dissociation inhibitor; GEF, guanine nucleotide exchange factor; PBS, phosphate-buffered saline; CM, conditioned medium.

differentiation, and apoptosis (13, 14). Recently, growing attention has been drawn toward the emerging role of the cytoskeleton in the modulation of apoptosis. RhoA, predominantly through its effectors ROCKI and ROCKII serine/threonine kinases, regulates the phosphorylation of multiple downstream targets, including myosin light chain and LIM kinases (15, 16), which control actin cytoskeleton assembly and cell contractility. It has been shown that caspase-3-mediated ROCKI activation is both necessary and sufficient for the formation of membrane blebs and nuclear disintegration in apoptotic cells (17, 18). In some cell types, ROCK is involved in the intracellular signaling that initiates apoptosis, such as caspase-8, caspase-10, and caspase-3 activation (19) or modulates the transcription of the proapoptotic proteins, such as Bax (20).

Emerging evidence implicated Rho GTPases as mediators of PKC signaling. For example, the decreased invasiveness of PKCϵ-depleted head and neck squamous carcinoma cells is associated with a corresponding inactivation of RhoA and RhoC GTPases (21). PKCs can modulate Rho function through either Rho-GEF activation or Rho-GDI inactivation (22, 23) or by direct association to Rho (24). However, it is not known whether Rho or its downstream effectors are implicated in PMA-induced apoptosis in prostate cancer cells.

In the present study, we show that PMA causes a strong and sustained activation of Rho and the formation of stress fibers via PKCδ. Notably, inhibition of Rho or its downstream effector ROCK impairs apoptosis triggered by PKC activation, suggesting a crucial role for Rho and ROCK downstream of PKCδ. We also found that ROCK mediates the induction of p21^{Cip1}, a necessary event for apoptosis induced by PMA. All of these effects depend on the integrity of the cytoskeleton, since agents that disrupt cytoskeleton organization markedly impaired apoptosis, JNK activation, and p21^{Cip1} induction by PMA.

EXPERIMENTAL PROCEDURES

Materials—PMA was purchased from LC Laboratories (Woburn, MA). 4′,6-Diamidino-2-phenylindole, cytochalasin, and blebbistatin were obtained from Sigma. Y-27632 and SP600125 were purchased from Calbiochem. GF 109203X was purchased from Biomol (Plymouth Meeting, PA). Rhodamine-phalloidin was purchased from Molecular Probes, Inc. (Eugene, OR). Microcystin-LR was purchased from Alexis Biochemicals (San Diego, CA). Cell culture reagents and media were from ATCC (Manassas, VA).

Cell Culture—LNCaP, C4-2, and CWR22 human prostate cancer cells were cultured in RPMI 1640 medium supplemented with 10% fetal bovine serum and penicillin (100 units/ml)-streptomycin (100 μg/ml) at 37 °C in a humidified 5% CO_2 atmosphere.

Adenoviral Infections—LNCaP cells in 6-well plates (~70% confluence) growing in RPMI 1640 medium supplemented with 2% fetal bovine serum were infected with an adenovirus (AdV) for a dominant negative RhoA mutant N19-RhoA or a GFP control AdV for 14 h at a multiplicity of infection of 10 plaque-forming units/cell. After removal of the AdV by extensive washing, cells were incubated for an additional 24 h in RPMI 1640 medium supplemented with 10% fetal bovine serum. Expression of the recombinant protein remained stable

throughout the duration of the experiment, as detected by Western blotting (data not shown).

Western Blot Analysis—Cells were harvested into lysis buffer containing 50 mM Tris-HCl, pH 6.8, 10% glycerol, 2% SDS, and 5% β-mercaptoethanol. Protein determinations were performed with the Bio-Rad Dc protein assay according to the instructions provided by the manufacturer. Equal amounts of protein (20 μg/lane) were subject to SDS-PAGE and transferred to polyvinylidene difluoride membranes. Membranes were blocked with 5% milk or 5% bovine serum albumin in 0.05% Tween 20, phosphate-buffered saline and then incubated with the first antibody overnight at 4 °C. Membranes were washed three times with 0.05% Tween 20 in PBS and then incubated with anti-mouse or anti-rabbit secondary antibodies conjugated to horseradish peroxidase (1:3000; Bio-Rad). Bands were visualized with the ECL Western blotting detection system.

The following primary antibodies were used: anti-PKCδ (Transduction Laboratories, Lexington, KY); anti-RhoA (Santa Cruz Biotechnology, Inc., Santa Cruz, CA); anti-actin (Sigma); anti-p21^{Cip1}, anti-phospho-JNK, anti-JNK, anti-phospho-p38 MAPK, and anti-p38 MAPK (Cell Signaling Technology, Beverly, MA); and anti-phospho-MYPT1 (myosin phosphatase target subunit 1)-Thr^{850} (Millipore, Billerica, MA). All antibodies were used at a 1:1000 dilution except for the anti-actin antibody, which was used at a 1:20,000 dilution.

Apoptosis Assays—The incidence of apoptosis was determined as we previously described (7). Briefly, cells were stained with 4′,6-diamidino-2-phenylindole (Sigma). Cells were trypsinized, mounted on glass slides, fixed in 70% ethanol, and then stained for 20 min with 1 mg/ml 4′,6-diamidino-2-phenylindole. Apoptosis was characterized by chromatin condensation and fragmentation when examined by fluorescence microscopy. The incidence of apoptosis in each preparation was analyzed by counting ~300 cells.

RNA Interference (RNAi)—21-bp double-stranded RNAs were purchased from Dharmacon Research, Inc. (Dallas, TX) or Ambion (Austin, TX) and transfected into LNCaP cells using the Amaxa Nucleofector (Amaxa Biosystems, Gaithersburg, MD) following the instructions provided by the manufacturer. Experiments were performed 48 h after transfection. The following targeting sequences were used: CCATGAGTTT-ATCGCCACCTT (PKCδ 1), CCATGTATCCTGAGT-GGAA (PKCδ 2), AACATACTGGCCTGGACTGTT (p21^{Cip1} 1), ATCGTCCAGCGACCTTCCTTT (p21^{Cip1} 2), GGTAGC-TCTAAGTTTTGAT (Sp1 1), and GGTCATTTCTTTGCT-TATG (Sp1 2). As a control RNAi, we used the Silencer® negative control 7 siRNA (Ambion).

Real Time PCR—RNA was extracted using TRIzol (Invitrogen). Two μg of RNA/sample were reverse transcribed using the First-Strand cDNA synthesis kit (Amersham Biosciences) following the instructions provided by the manufacturer. PCR primers and fluorogenic probes for p21^{Cip1} were purchased from Applied Biosystems. The probes were 5′-end-labeled with 6-carboxyfluorescein. Each PCR amplification was performed in a total volume of 12.5 μl, containing 6.25 μl of 2× TaqMan Universal PCR Master Mix (Applied Biosystems), commercial target primers (300 nM), the fluorescent probe (200 nM),

and 1 μl of cDNA, using an ABI PRISM 7700 detection system. PCR product formation was continuously monitored using Sequence Detection System software version 1.7 (Applied Biosystems). The 6-carboxyfluorescein signal was normalized to endogenous 18 S RNA.

Plasmid Transfections and Promoter Analyses—LNCaP cells (1.5×10^6 cells) were transfected with 2 μg of p21^{Cip1} firefly luciferase reporter vectors (25) using the Amaxa Nucleofector. A *Renilla* luciferase expression vector (100 ng, pRL-TK; Promega, Madison, WI) was co-transfected for normalization of transfection efficiency. Forty-eight h after transfection, cells were stimulated with PMA and lysed. Cell extracts were subject to luciferase determination using the Dual-Luciferase reporter assay system (Promega).

Confocal Microscopy and Phalloidin Staining—Cells were washed twice with PBS, fixed in 4% paraformaldehyde in PBS for 10 min, and washed briefly with PBS. For phalloidin staining, cells were blocked in 5% bovine serum albumin in PBS for 30 min. Cells were stained with phalloidin (Molecule Probes) in PBS containing 1% bovine serum albumin (30 min, room temperature) and then stained with 4′,6′-diamidino-2-phenylindole (1 μg/ml, 20 min, 4 °C). For the determination of GFP-PKCδ localization, LNCaP cells were transfected with pEGFP-PKCδ plasmid using the Amaxa Nucleofector and 48 h later treated with PMA. In all cases, coverslides were mounted with Fluoromount-G (SouthernBiotech) and visualized with a laser-scanning fluorescence microscope (LSM 410 or 510; Carl Zeiss).

RhoA Activation Assay—RhoA-GTP levels were determined with a pull-down assay using the rhotekin binding domain and detected by Western blot with an anti-RhoA antibody (26). Briefly, cells were lysed in a buffer containing 50 mM Tris-HCl, pH 7.2, 1% Triton X-100, 0.5% sodium deoxycholate, 0.1% SDS, 500 mM NaCl, and 10 mM MgCl$_2$. The supernatant was collected and incubated with glutathione *S*-transferase-rhotekin binding domain (20 μg) for 60 min at 4 °C. Beads were washed with 50 mM Tris-HCl buffer containing 1% Triton X-100, 150 mM NaCl, 10 mM MgCl$_2$, boiled with SDS sample buffer with 5% 2-mercaptoethanol, and subjected to Western blot.

ROCK Kinase Assays—ROCK kinase activity was measured by two approaches. First, we determined phosphorylation of the endogenous ROCK substrate MYPT1 in total cell extracts using a rabbit anti-phospho-Thr^{850}-MYPT1 antibody (27). Second, we used the ROCK Activity Immunoblot Kit (Cell Biolabs, Inc.). Briefly, cells were washed twice with ice-cold PBS and lysed with an immunoprecipitation buffer (50 mM HEPES, pH 7.4, 150 mM NaCl, 1 mM MgCl$_2$, 10 mM NaF, 5% glycerol, 1% Nonidet P-40, 1 mM dithiothreitol, 1 mM EGTA, 1 μM microcystin-LR, and mixture proteinase inhibitor). Cell lysates were centrifuged at 10,000 rpm for 10 min to remove insoluble debris. Supernatants were transferred to fresh tubes, precleared with protein G-Sepharose (Invitrogen) beads for 15 min, and incubated with an anti-ROCK antibody (Santa Cruz Biotechnology) for 40 min. The antibody-ROCK complexes were pulled down with protein G-Sepharose beads (20 min). Beads were washed three times in immunoprecipitation buffer and incubated with the kinase reaction mixture (final volume = 25 μl) that included 0.25 μg of rMYPT1 and 200 μg of ATP, fol-

lowing the protocol indicated by the manufacturer. Samples were subjected to Western blot, and rMYPT1 phosphorylation was determined using a rabbit anti-phospho-Thr^{850} MYPT1 antibody.

Enzyme-linked Immunosorbent Assay—TNFα levels were determined by ELISA (Pepro Tech Inc.), essentially as described previously (11). Briefly, 100 μl of conditioned medium (CM) were added into each well and incubated overnight at 4 °C. Subsequently, 100 μl of biotin-labeled anti-TNFα antibody (0.25 μg/ml) was added for 2 h at room temperature. Bound antibody was detected by incubation with peroxidase-labeled avidin and 2,2′-azino-bis(3-ethylbenzothiazoline-6-sulfonic acid) from Sigma, and absorbance was measured at 450 nm. Nonspecific binding was blocked with 1% bovine serum albumin in PBS.

RESULTS

PMA Induces the Activation of Rho and ROCK in LNCaP Prostate Cancer Cells—Phorbol esters induce a strong apoptotic response in LNCaP cells. This effect is mediated primarily by PKCδ, which upon activation stimulates the release of death factors and the extrinsic apoptotic cascade (11). Since PKC isozymes have been shown to regulate Rho GTPases, and Rho has been implicated in apoptosis triggered by diverse stimuli, we speculated that this small G-protein could be involved in phorbol ester-induced apoptosis in prostate cancer cells. To address this issue, we first examined if PMA could promote the activation of RhoA in LNCaP cells. Using a pull-down assay, we found that treatment with PMA (100 nM) caused a robust and sustained elevation in Rho-GTP levels in LNCaP cells, which persisted for at least 3 h poststimulation (Fig. 1A). RhoA activation by PMA was blocked by pretreatment of LNCaP cells with the pan-PKC inhibitor GF 109203X (Fig. 1B), suggesting that it is mediated by PKC isozymes and not other phorbol ester receptors unrelated to PKC (2).

Since ROCK is a main Rho effector, we determined the effect of PMA on ROCK activation in LNCaP cells. As a first approach, we examined the phosphorylation of the ROCK substrate MYPT1, using a specific phosphoantibody against Thr^{850}-MYPT1, a well established ROCK phosphorylation site (27). As shown in Fig. 1C (*left*), PMA induces a marked MYPT1 phosphorylation, which peaks at 15 min and is sustained for at least 1 h. ROCK activation can also be observed in C4-2 and CRW22 androgen-dependent prostate cancer cells (Fig. 1C, *right*).

Next, we examined ROCK activation using an immunoprecipitation assay. Endogenous ROCK was pulled down from LNCaP cells treated with PMA (100 nM, 0–15 min), and ROCK activity was determined using an *in vitro* kinase assay using as a substrate the recombinant fragment of MYPT1 that comprises the ROCK phosphorylation site (amino acids 654–880). Phosphorylation of the peptide was determined by Western blot using the anti-Thr^{850}-MYPT1 antibody. Consistent with the results in Fig. 1C, ROCK kinase activity was enhanced in immunoprecipitates of PMA-treated LNCaP cells (Fig. 1D). Activation of ROCK by PMA was blocked by pretreatment of cells with the ROCK inhibitor Y-27632 (Fig. 1E), as expected, as well as by the pan-PKC inhibitor GF 109203X (Fig. 1F).
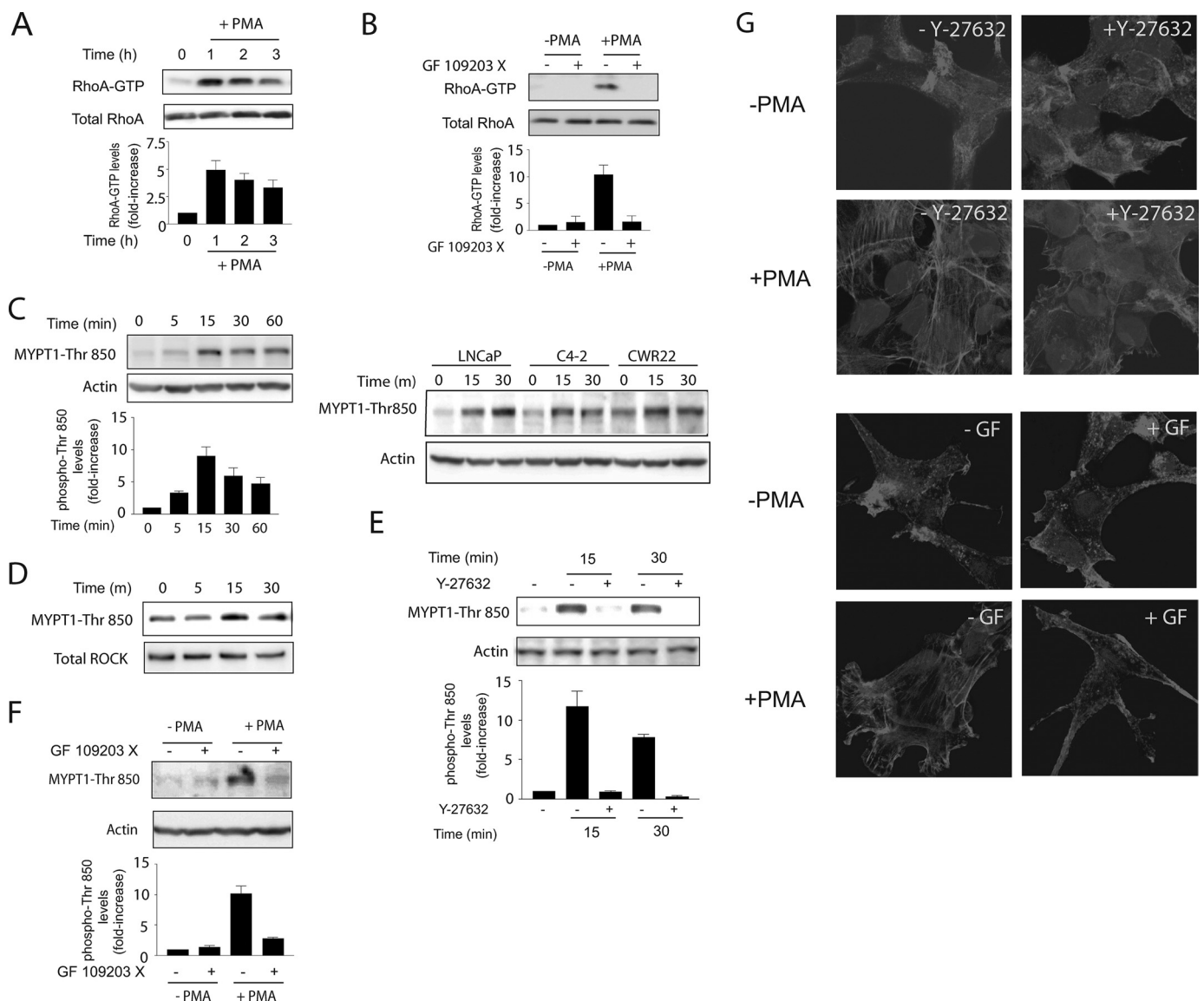
FIGURE 1. **PMA activates Rho and ROCK in LNCaP cells.** *A*, LNCaP cells were treated with PMA (100 nM) for 1 h, and cell lysates were collected at different times. Rho-GTP levels were determined using a pull-down assay. *B*, effect of the PKC inhibitor GF 109203X (5 μM) on RhoA activation. The inhibitor was added 45 min before and during PMA or vehicle (ethanol) treatment. *C* (*left*), LNCaP cells were treated with PMA (100 nM) for different times, and MYPT1-Thr850 phosphorylation was determined in cell extracts by Western blot. A densitometric analysis is presented. *Right*, comparison of different prostate cancer cell lines. *D*, LNCaP cells were treated with PMA (100 nM), and at different times, ROCK activity was determined in immunoprecipitates. *E*, effect of the ROCK inhibitor Y-27632 (10 μM) on PMA-induced MYPT1-Thr^{850} phosphorylation in cell extracts. *F*, effect of the PKC inhibitor GF 109203X (5 μM) on PMA-induced MYPT1-Thr^{850} phosphorylation in cell extracts. For *A–C*, *E*, and *F*, densitometric analysis is presented in each case as mean ± S.D. (*n* = 3). *G*, LNCaP cells were treated with PMA (+*PMA*; 100 nM) or vehicle (−*PMA*) for 30 min and subjected to phalloidin staining. Cells were visualized by confocal microscopy. Experiments were carried out in the presence of GF 109203X (5 μM) or Y-27632 (10 μM). Similar results were observed in at least three experiments.

Rho GTPases are best known for their roles in the regulation of cytoskeleton rearrangement and the generation of the contractile force necessary for the formation of stress fibers (13). We first examined if PKC activation causes cytoskeleton reorganization in LNCaP cells. As shown in Fig. 1*G*, PMA promotes the formation of stress fibers, and this effect was sensitive to the PKC inhibitor GF 109203X. Moreover, the ROCK inhibitor Y-27632 blocked the formation of stress fibers in response to PMA. Taken together, these results indicate that PMA is a strong activator of Rho and its downstream effector ROCK in LNCaP prostate cancer cells.

Rho and ROCK Are Implicated in PMA-induced Apoptosis— To determine whether Rho plays a role in PMA-induced apo-

ptosis in LNCaP cells, we expressed a dominant negative RhoA mutant (N19-RhoA) by adenoviral means. As a control, we used a GFP AdV. Expression of N19-RhoA reduced the apoptotic effect of PMA by ~40% (Fig. 2*A*). Next, to determine if ROCK is implicated in PMA-induced apoptosis, we used the ROCK inhibitor Y-27632. As shown in Fig. 2*B*, the ROCK inhibitor significantly blocked PMA-induced apoptosis in LNCaP cells, suggesting a role for the Rho-ROCK pathway in phorbol ester-induced apoptosis. Y-27632 also blocked the apoptotic effect of PMA in C4-2 and CRW22 cells (supplemental Fig. S1).

*PKCδ Mediates PMA-induced Activation of Rho and Stress Fiber Formation—*Previous studies from our laboratory demonstrated that PMA-induced apoptosis is mediated by the acti-
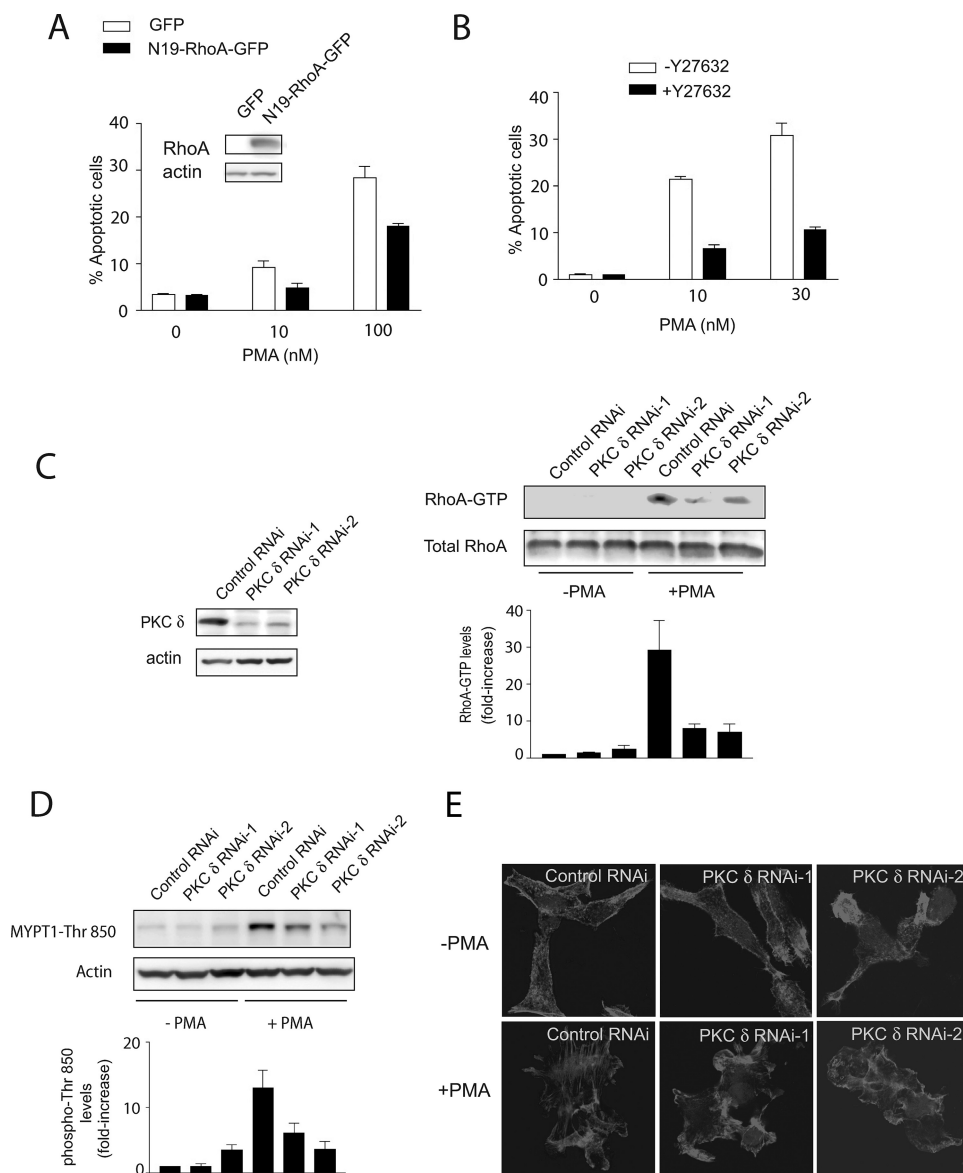
FIGURE 2. **Activation of PKCδ is required for RhoA and ROCK activation, stress fiber formation, and PMA-induced apoptosis in LNCaP cells.** *A*, LNCaP cells were infected with AdVs for either dominant negative RhoA (N19-RhoA) or a control AdV (GFP), using a multiplicity of infection of 10 plaque-forming units/cell. After 14 h, AdVs were removed by extensive washing, and cells were grown in complete medium for 48 h. Cells were then treated with PMA (10–100 nM, 1 h), and the incidence of apoptosis was determined 24 h later. *Inset*, expression of N19-RhoA by Western blot. *B*, LNCaP cells were treated with the ROCK inhibitor Y-27632 (10 μM), added 1 h before PMA treatment. Cells were treated with PMA (10–30 nM, 1 h), and the incidence of apoptosis was determined 24 h later. *C*, LNCaP cells were transfected with RNAi duplexes for PKCδ or a control RNAi. After 48 h, cells were treated with PMA (+*PMA*; 100 nM, 1 h) or vehicle (−*PMA*), and Rho-GTP levels were determined 1 h later. Densitometric analysis of three independent experiments is shown, expressed as mean ± S.D. (n = 3). *Left*, expression of PKCδ by Western blot. *Right*, representative experiment. *D*, LNCaP cells subject to PKCδ RNAi depletion were treated with PMA (+*PMA*; 100 nM) or vehicle (−*PMA*) for 15 min, and MYPT1-Thr850 phosphorylation levels in cell extracts were determined by Western blot. For *A–D*, the corresponding densitometric analysis is presented, expressed as mean ± S.D. (n = 3). *E*, LNCaP cells subject to PKCδ RNAi depletion were treated with PMA (+*PMA*; 100 nM) or vehicle (−*PMA*) for 30 min and stained with phalloidin. Cells were visualized by confocal microscopy. Similar results were observed in at least three independent experiments.

this PKC is implicated in Rho activation by PMA. RhoA-GTP levels were determined in LNCaP cells subject to PKCδ RNAi, using two different RNAi duplexes (PKCδ RNAi-1 and PKCδ RNAi-2). PKCδ depletion was >75% with either RNAi duplex (Fig. 2*C*, *left*). Fig. 2*C* (*right*) shows that the activation of RhoA by PMA was greatly reduced in PKCδ-depleted LNCaP cells. We next assessed the effect of PKCδ knockdown on ROCK activation. As shown in Fig. 2*D*, PMA-induced activation of ROCK in LNCaP cells was impaired as a consequence of PKCδ RNAi depletion. To further assess the involvement of PKCδ in Rho function, we examined stress fiber formation in response to PMA in PKCδ-depleted cells. Fig. 2*E* shows that LNCaP cells subjected to PKCδ RNAi failed to assemble stress fibers in response to the PKC activator. These observations indicate that activation of PKCδ in LNCaP cells promotes the activation of RhoA and RhoA-dependent responses via ROCK.

Cytoskeleton-dependent JNK Activation Is Required for PMA-induced Apoptosis—Our previous studies established that the apoptotic effect of phorbol esters is caused by the autocrine release of death factors, primarily TNFα and TRAIL, an effect mediated by PKCδ. CM collected from PMA-treated LNCaP cells has the ability to trigger an apoptotic response via the extrinsic cascade, which becomes activated in response to the death factors released to the CM. Although we found that inhibition of JNK does not affect the release of death factors (11), SP600126 blocked the apoptotic effect of CM from PMA-treated cells, suggesting a key role for the JNK pathway in the effect of the autocrine factors. CM collected from PMA-

vation of PKCδ. Inhibition of PKCδ by either pharmacological means or expression of a dominant negative PKCδ mutant reduces PMA-induced apoptosis in LNCaP cells (7, 11, 28). Likewise, we reported that PKCδ depletion from LNCaP cells using RNAi markedly impairs the apoptotic response of the phorbol ester (11).

Given the involvement of PKCδ as a mediator of phorbol ester-induced apoptosis (7, 11, 28), we decided to evaluate if

treated LNCaP cells causes a strong and sustained JNK activation when added to a previously untreated culture of LNCaP cells (11). Fig. 3*A* shows that the JNK inhibitor SP600126 caused a significant impairment of the PMA apoptotic response. The effect was observed when SP600126 was left in the medium after the PMA treatment but not if only added for short times after PMA treatment (data not shown) (28). These results are consistent with the involvement of JNK as a mediator of the effect of death factors but
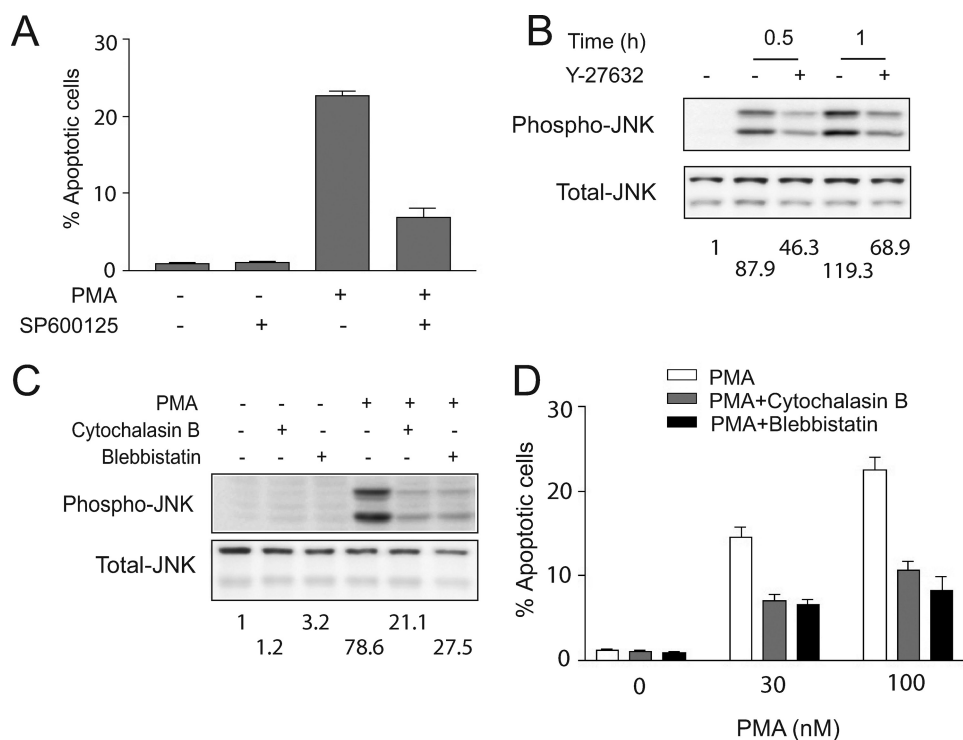
FIGURE 3. **ROCK-mediated JNK activation is required for PMA-induced apoptosis.** *A*, LNCaP cells were treated with SP600125 (20 μM), added 1 h before PMA (100 nM, 1 h) or vehicle (ethanol) treatment. The incidence of apoptosis was determined 24 h later. *B* and *C*, LNCaP cells were treated with Y-27632 (10 μM) (*B*), cytochalasin B (2 μM), or blebbistatin (50 μM) (*C*), added 1 h before PMA treatment. Cells were then treated with 100 nM PMA for the indicated times (*B*) or for 30 min (*C*), and phospho-JNK or total JNK levels were determined by Western blot. The -fold increase in phospho-JNK levels is shown *below* the corresponding Western blots. *D*, LNCaP cells were treated with cytochalasin B (2 μM) or blebbistatin (50 μM), added 1 h before PMA or vehicle (ethanol) treatment. Cells were treated with PMA (30–100 nM) or vehicle for 1 h. The incidence of apoptosis was determined 24 h later. Results are presented as mean $\pm$ S.D. ($n = 3$). Two additional experiments gave similar results.

not their release (11). It has been demonstrated in various cellular models that Rho and ROCK mediate JNK activation in response to stimuli (29–31). Therefore, we examined if ROCK is involved in JNK activation by PMA in LNCaP cells. As shown in Fig. 3*B*, the ROCK inhibitor Y-27632 markedly reduced JNK activation.

ROCK plays a major role in the assembly of actin stress fibers, which is required for membrane blebbing and nuclear disintegration and has been shown in some cases to be required for the execution of apoptosis (13–19). These effects are mediated by ROCK phosphorylation of myosin light chain and activation of its ATPase activity, thus increasing the actin-myosin force and cell contractility (15, 18). We therefore speculated that the cytoskeleton is implicated in apoptosis triggered by PKCδ activation. To address this issue, we used the actin-destabilizing agent cytochalasin B and the myosin II inhibitor blebbistatin. As shown in Fig. 3*C*, although cytochalasin B or blebbistatin did not cause any measurable apoptotic response by themselves, they markedly inhibit PMA-induced apoptosis in LNCaP cells. This suggests that cytoskeleton rearrangement in response to PMA activation is required for the apoptotic effect of the phorbol ester in LNCaP prostate cancer cells. Furthermore, the cytoskeleton inhibitors cytochalasin B and blebbistatin also blocked JNK activation by PMA (Fig. 3*D*). Inhibition of cytoskeleton reorganization did not impair PKCδ activation, as determined by the lack of effect of blebbistatin on PKCδ trans-

location (supplemental Fig. S2). Taken together, these results indicate that ROCK regulates apoptosis through the activation of the JNK pathway through a cytoskeleton-dependent mechanism.

ROCK-mediated p21^{Cip1} Up-regulation Is Required for Apoptosis— It is noteworthy that in many cell types, PKC activation leads to the induction of the cell cycle inhibitor p21^{Cip1}, which plays a central role in PMA-induced cell cycle arrest and senescence. This induction could be either p53-dependent or p53-independent, depending upon the cell type and stimuli (4, 32, 33). Studies have shown that p21^{Cip1} up-regulation preceded apoptosis induced by PMA in prostate cancer cells. To determine whether a causal relationship between p21^{Cip1} and PMA-induced apoptosis exists, we knocked down p21^{Cip1} using two different RNAi duplexes (p21 RNAi-a and p21 RNAi-b). A significant depletion in p21^{Cip1} levels was observed by delivery of either RNAi duplex into LNCaP cells (Fig. 4*A*). In LNCaP cells subjected to p21^{Cip1} RNAi, the induction of this cell cycle inhibitor was significantly attenu-

ated, although full inhibition of p21^{Cip1} up-regulation could not be achieved ($\sim$70–80% depletion). Knockdown of p21^{Cip1} led to a reduced PMA apoptotic response (Fig. 4*B*). The effect was partial, which may suggest a partial requirement for p21^{Cip1} or otherwise relate to the residual p21^{Cip1} induction by the phorbol ester. The requirement of p21^{Cip1} for phorbol ester-induced apoptosis prompted us to investigate whether this effect was ROCK-mediated. We therefore examined the effect of Y-27632 on p21^{Cip1} induction. Fig. 4*C* shows that PMA treatment caused a time-dependent induction of p21^{Cip1} in LNCaP cells. This induction was markedly reduced in the presence of the ROCK inhibitor (see also Fig. 4*E*). To determine whether p21^{Cip1} up-regulation by PMA is dependent upon the cytoskeleton rearrangement, we examined the effect of cytochalasin B and blebbistatin. Interestingly, both cytoskeleton inhibitors prevented p21^{Cip1} up-regulation by the phorbol ester (Fig. 4*D*). The induction of p21^{Cip1} by PMA was not affected by the JNK inhibitor SP600125 (Fig. 4*E*), suggesting that JNK activation and p21^{Cip1} induction downstream of Rho/ROCK are implicated in parallel mechanisms rather than in a linear pathway.

ROCK Regulates p21^{Cip1} at a Transcriptional Level—Expression of p21^{Cip1} is controlled both by transcriptional and post-transcriptional mechanisms, including in response to PMA (4, 32, 33). Previous studies from our laboratory established a key role for PKCδ in p21^{Cip1} induction. PMA caused a marked ele-
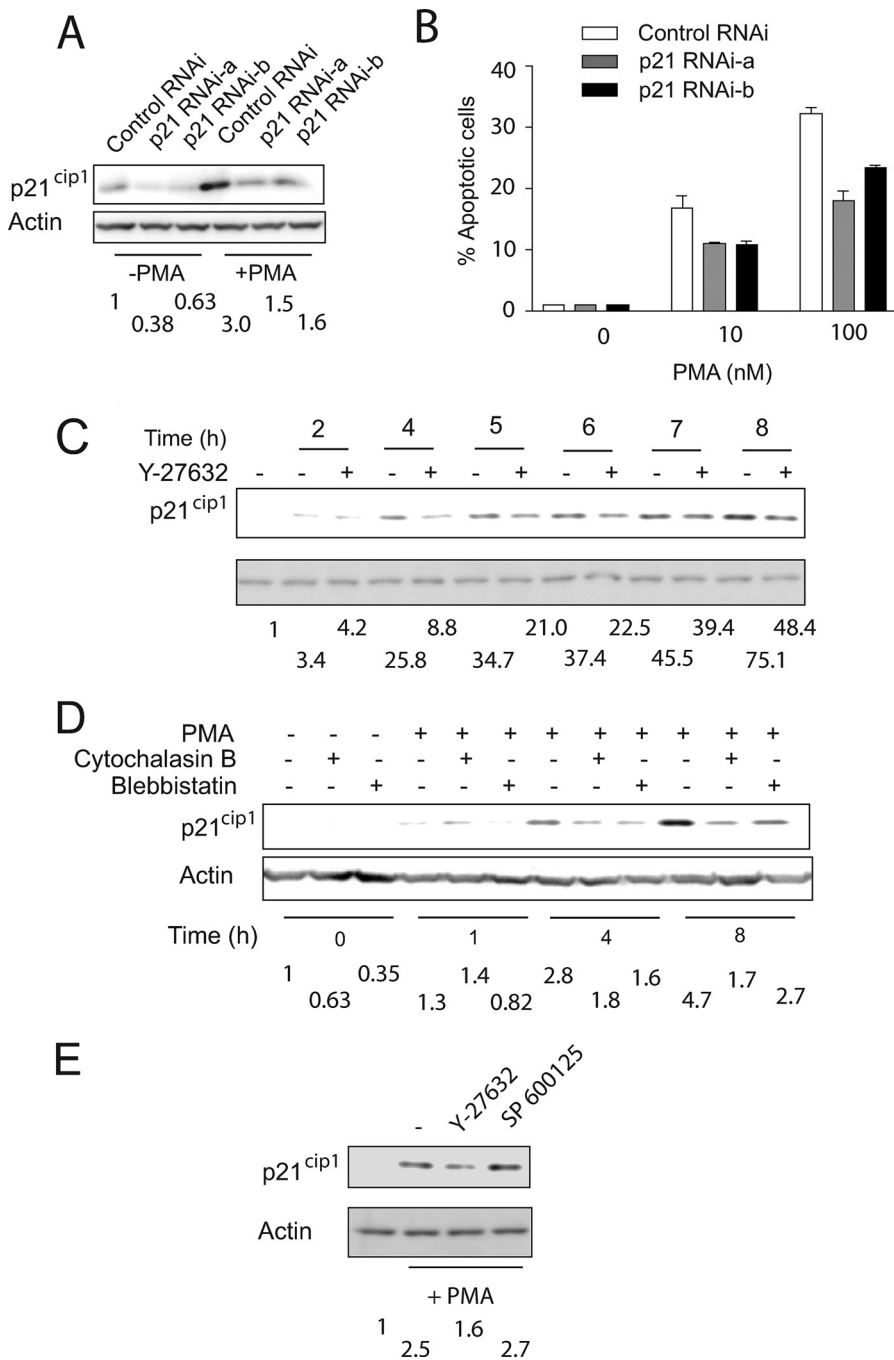
FIGURE 4. **ROCK mediated p21^{Cip1} up-regulation is required for PMA-induced apoptosis.** *A*, LNCaP cells were transfected with p21^{Cip1} RNAi duplexes or control RNAi and 48 h later treated with 100 nM PMA for 1 h. p21^{Cip1} levels were determined 8 h later by Western blot. *B*, 48 h after transfection with the different RNAi duplexes, cells were treated with either PMA (10 or 100 nM) or vehicle (ethanol) for 1 h. The incidence of apoptosis was determined 24 h later. Results are presented as mean ± S.D. (*n* = 3). Two additional experiments gave similar results. *C* and *D*, LNCaP cells were treated with Y-27632 (10 μM) (*C*), cytochalasin B (2 μM), or blebbistatin (50 μM) (*D*) and 1 h later incubated with 100 nM PMA for 1 h. Cell extracts were prepared at the indicated times, and p21^{Cip1} levels were determined by Western blot. *E*, LNCaP cells were treated with Y-27632 (10 μM) or SP600125 (20 μM) or SB203580 (10 μM) for 1 h before PMA treatment. Cells were then treated with 100 nM PMA for 1 h and collected at 9 h after PMA treatment. p21^{Cip1} in cell extracts were subject by Western blot. Similar results were observed in at least three independent experiments. For *A* and *C–E*, the -fold changes in p21^{Cip1} levels are shown *below* the corresponding Western blots.
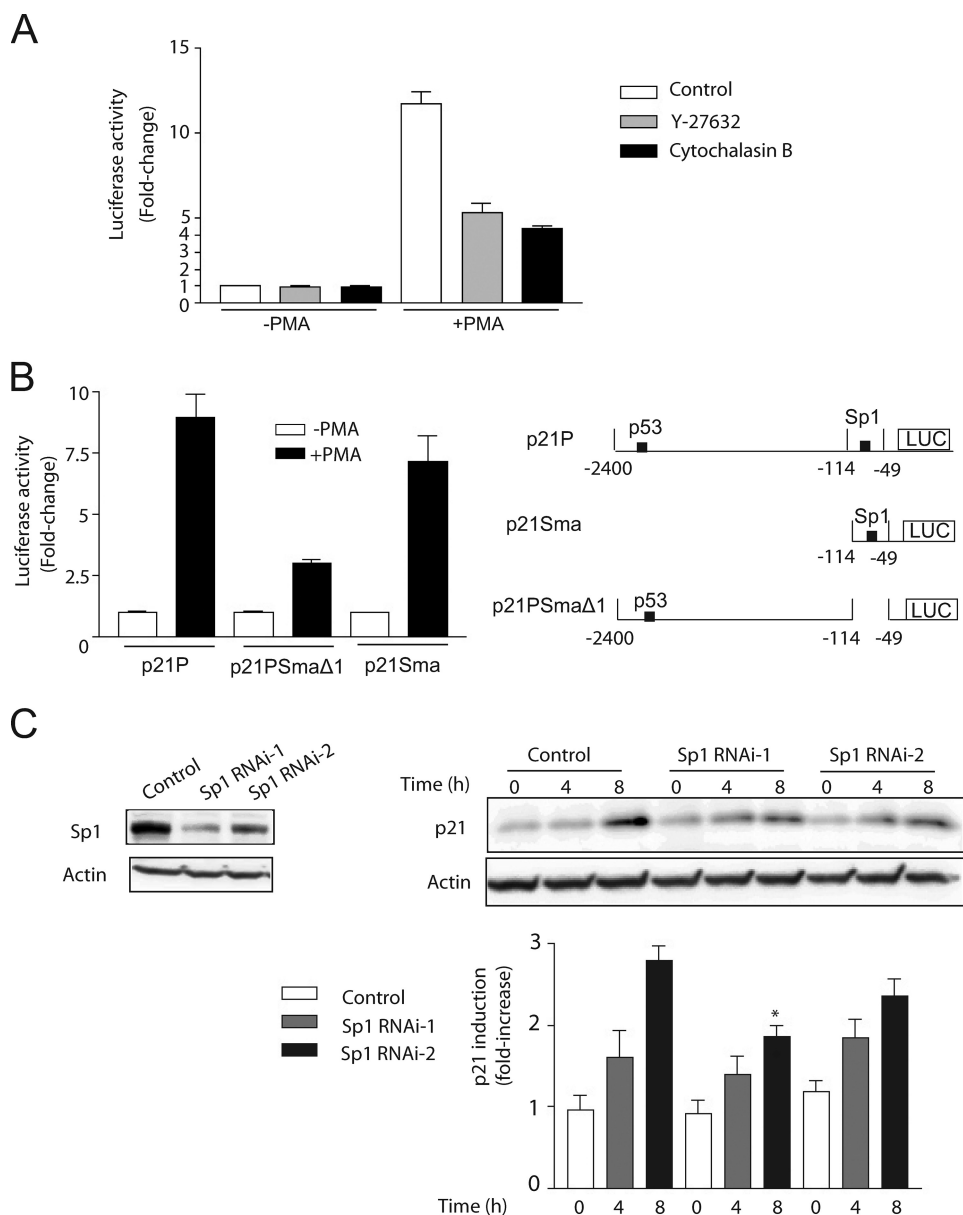
using a p21^{Cip1} promoter luciferase reporter. LNCaP cells were transfected with the p21^{Cip1} reporter vector p21P (25), which encodes a fragment comprising bp −1 to −2400 in the human p21^{Cip1} promoter fused to firefly luciferase. A *Renilla* luciferase vector was co-transfected for normalization of transfection efficiency. As shown in Fig. 5*A*, PMA treatment led to a marked increase in luciferase activity. Treatment with either Y-27632 or cytochalasin inhibited luciferase activity to a great extent.

Transcriptional activation of p21^{Cip1} is mediated through multiple mechanisms. Among the most relevant transcription factors, p53 and Sp1 have been widely implicated in transcriptional control of the p21^{Cip1} promoter (32, 34, 35). We used two deletion mutants of the human p21^{Cip1} promoter. The first mutant (p21PSma) has a deletion in bp −114 to −2400, which comprises the p53-responsive element in the promoter. The second mutant (p21PSmaΔ1) has the four Sp1 elements deleted (deletion in bp −49 to −114). Notably, although deletion of the large fragment that includes the p53-binding site caused only a minimal effect, deletion of the Sp1-responsive elements abrogated the induction of luciferase activity by PMA (Fig. 5*B*). To demonstrate the involvement of Sp1 in p21^{Cip1} induction, we used RNAi to knock down endogenous Sp1. We used two RNAi sequences: Sp1 RNAi-1, which depleted endogenous Sp1 by >80%, and Sp1 RNAi-2, which was less efficient (Fig. 5*C*, *left*). We found that Sp1 RNAi-1 significantly blocked p21^{Cip1} up-regulation, whereas Sp1 RNAi-2 had only a marginal effect (Fig. 5*C*, *right*). These results suggest that the induction of p21^{Cip1} by PMA is mediated by Sp1-dependent mechanisms and independent of p53, despite the fact that LNCaP cells have functional p53.

ROCK Regulates TNFα Secretion in a JNK-independent Manner—Previous studies from our laboratory demonstrated that PMA-induced apoptosis of LNCaP cells is triggered by the autocrine secretion of death factors via PKCδ, with the subse-

vation in p21^{Cip1} mRNA levels, as determined by real time PCR (4.0 ± 0.9-fold increase at 3 h; 7.9 ± 0.6-fold increase at 6 h; *n* = 3). To determine whether p21^{Cip1} induction by PMA has a transcriptional component, we carried out a gene reporter assay

FIGURE 5. **PMA induces p21^{Cip1} mRNA levels and activates a human p21^{Cip1} luciferase reporter.** *A*, LNCaP cells were co-transfected with a p21^{Cip1} firefly luciferase reporter and pTK-*Renilla*. Forty-eight h later, cells were treated with either 100 nM PMA or vehicle for 1 h, in the presence of Y-27632 (10 μM) or cytochalasin B (2 μM). Luciferase activity was determined at 9 h after PMA treatment and normalized to *Renilla* luciferase activity. *B*, LNCaP cells were co-transfected with p21^{Cip1} firefly luciferase reporters with different deletions in the promoter region and pTK-*Renilla*. Forty-eight h later, cells were treated with either 100 nM PMA or vehicle for 1 h. Luciferase activity was determined at 9 h after PMA treatment and normalized to *Renilla* luciferase activity. Results are expressed as -fold change relative to vehicle-treated cells and presented as mean $\pm$ S.D. ($n = 3$). Similar results were observed in three experiments. *C*, LNCaP cells subject to Sp1 RNAi depletion were treated with 100 nM PMA for 1 h, and p21^{Cip1} induction was determined by Western blot. *Left*, representative Sp1 depletion. *Upper right*, representative p21^{Cip1} induction. *Lower right*, densitometric analysis of three independent experiments, expressed as mean $\pm$ S.D. *, $p < 0.05$ *versus* control, 8 h.

quent activation of the extrinsic apoptotic cascade. Among the death factors, TNFα is the most relevant one. JNK was identified as a mediator of the TNFα effect (11). To examine whether ROCK regulates TNFα secretion via JNK, we compared TNFα levels in conditioned medium from LNCaP cells treated with PMA in the absence or presence of the ROCK inhibitor Y-27632 or the JNK inhibitor SP600125. As shown in Fig. 6*A*, ROCK inhibitor markedly inhibited TNFα secretion, whereas

the JNK inhibitor had no effect. These results suggest that ROCK regulates TNFα secretion in a JNK-independent manner.

DISCUSSION

Despite the well established role for PKC in mitogenesis and tumor promotion, considerable evidence supports the involvement of discrete PKC isozymes in growth inhibition and apoptosis. Phorbol esters exert profound effects on the machinery that controls the cell cycle and modulate in either positive or negative manners multiple signaling pathways implicated in proliferation, survival, and apoptosis. In that regard, studies by our laboratory and others have established a prominent role for PKCδ, a member of the novel PKC family, as a mediator of growth inhibition and apoptosis in response to phorbol esters (4–8, 11, 28). Androgen-dependent prostate cancer cells, such as LNCaP and CWR22-Rv1 cells, undergo apoptosis in response to phorbol esters via activation of PKCδ (7–9). The signaling components implicated in PKCδ-driven apoptosis are only partially understood. Previous studies from our laboratory established key roles for the JNK cascade as a mediator of phorbol ester-induced apoptosis in LNCaP cells (11, 28). A more detailed analysis established that apoptosis is triggered by the autocrine secretion of death factors from prostate cancer cells via PKCδ, including TNFα and TRAIL, with the subsequent activation of the extrinsic apoptotic cascade. Interfering with death receptor signaling either by inhibition/depletion of TNFα/TRAIL receptors, RNAi depletion of the adaptor FADD or caspase-8, or pharmacological inhibition of p38 MAPK and JNK pathways in all cases impairs phorbol ester-induced apoptosis (11). A distinctive aspect of the present study is the identification of the Rho-ROCK-p21^{cip1} pathway as an effector of PMA-induced apoptosis, which provides an additional layer of complexity and argues for the involvement of an intricate network of signaling cascades in this effect.

Our results provide evidence that PMA induces RhoA and ROCK activation as well as the formation of stress fibers in
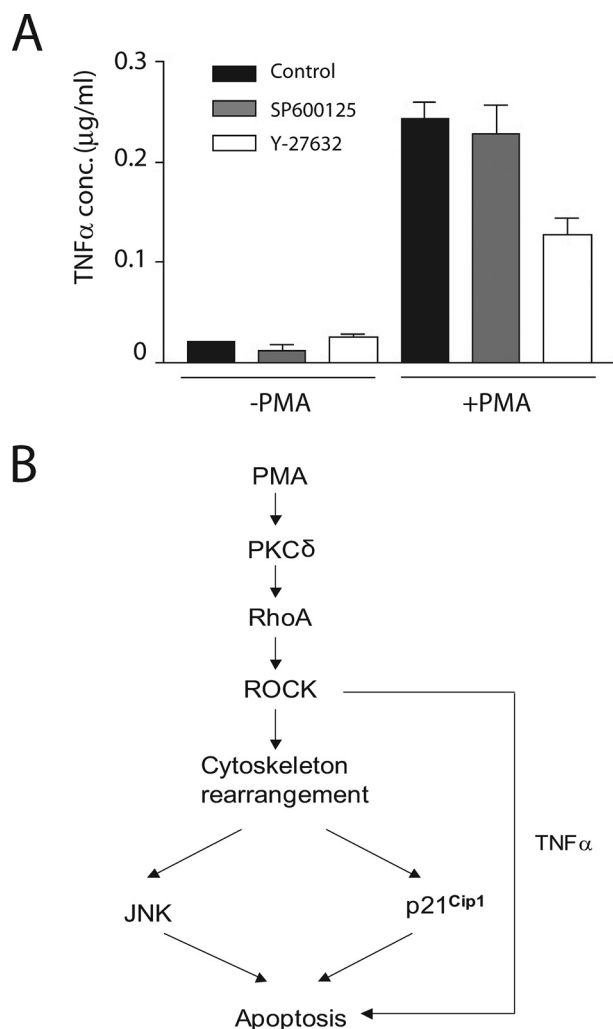
FIGURE 6. **ROCK regulates TNFα secretion in a JNK-independent manner.** *A*, LNCaP cells were treated with either PMA (+*PMA*) or vehicle (−*PMA*) in the absence or presence of the ROCK inhibitor Y-27362 (10 μM) or the JNK inhibitor SP600125 (25 μM). Conditioned medium was collected after 24 h, and TNFα levels were determined by an enzyme-linked immunosorbent assay. Results are presented as mean ± S.D. of triplicate samples. Similar results were obtained in an additional experiment. *B*, a model summarizing our findings.

LNCaP prostate cancer cells via ROCK. The activation of the Rho pathway and cytoskeletal organization by PMA is mediated by PKCδ. Both the pan-PKC inhibitor GF 109203X and PKCδ RNAi depletion block RhoA activation and stress fiber formation. PKC isozymes have been implicated in Rho activation in several models, including cardiomyocytes (36), myoblasts (37), and endothelial cells (38). Although the mechanistic basis of PKCδ modulation of Rho/ROCK function in LNCaP still remains to be elucidated, it has been shown that phorbol esters can activate Rho GTPases through different mechanisms that involve either Rho-GEF activation or Rho-GDI inactivation (22, 23). Rho-GEFs are a very diverse family, with >70 members being identified in humans (39). Studies have shown that PMA-induced apoptosis in erythroblastic D2 cells involves the RhoA-GEF GEF-H1. Depletion of GEF-H1 leads to a significant reduction of RhoA activity and prevents cells from undergoing PMA-induced apoptosis via the Rho-ROCK pathway (22). Studies in vascular smooth muscle cells revealed that Rho-dependent

migration and JNK activation induced by angiotensin II were inhibited by the PKCδ inhibitor rottlerin or a dominant negative PKCδ mutant. PKCδ-dependent Rho/ROCK activation in these cells possibly involves PDZ-RhoGEF (40). There is also evidence that a PKC phosphorylation site in Rho-GDI modulates its association/dissociation from RhoA by changing the affinity for the small G-protein. Upon phosphorylation in Ser[96], Rho-GDI dissociates from RhoA, thereby enabling RhoA activation in response to stimuli (23). Conceivably, PKCδ may also regulate the activity of Rho-GAPs and control the rate of GTP hydrolysis from the GTPase. For example, phorbol esters stimulate the phosphorylation of the Rho-GAP DLC1, leading to its relocalization and suppression of GAP activity. Several studies have also reported a physical association between PKCs and RhoA (24, 41). Although there is very limited information regarding the expression and regulation of Rho-GEFs in prostate cancer cells, it is conceivable that mechanisms such as those described above and/or alternative yet unknown mechanisms may operate in prostate cancer cells, which requires further investigation, since they should provide relevant information on how PKCδ modulates RhoA in the context of apoptotic responses. Candidate Rho GEFs include Vav3, which has been implicated in prostate cancer progression (42), as well as LARG and PDZ-Rho-GEF, which mediate downstream Rho signaling in prostate cancer models (43, 44).

ROCK is a major regulator of cytoskeleton reorganization in response to stimuli. Studies have implicated the Rho/ROCK pathway in apoptosis in various cell models, including prostate cancer cells (19, 45), and established links between cytoskeleton remodeling and apoptosis programming or execution (17–19). ROCK has been implicated in myosin light chain phosphorylation and membrane blebbing as well as in Golgi fragmentation during apoptosis (47, 48). It is also known that ROCK modulates the extrinsic apoptotic cascade, which mediates PMA-induced apoptosis in LNCaP prostate cancer cells via the autocrine release of death factors and activation of caspase-8 (11). Studies in a paradigm of PMA-induced apoptosis in erythroblastic TF-1 cells implicated ROCK in the formation of DISC complex (19). Interestingly, we also found that ROCK inhibition prevents the release of death factors from LNCaP cells in response to PMA (data not shown). Since this release of death factors is entirely dependent on PKCδ (11), we speculate that ROCK is also downstream of PKCδ in the regulation of the autocrine response. Studies have shown that the cytoskeleton is involved in the extrinsic apoptotic cascade, since it controls DISC formation and modulates the localization of key components of the cascade, including death receptors (49–51). The Rho pathway also controls transcriptional mechanisms via cytoskeleton-dependent and -independent processes (29, 52, 53), and a ROCK-dependent transcriptome has been recently defined, which includes genes involved in cytoskeletal reorganization (54). Actin polymerization modulates the activity of RNA polymerases and has been also implicated in chromatin remodeling as well, since it serves as a platform for the co-transcriptional recruitment and/or tethering of histone-modifying enzymes via its association with pre-mRNPs (55). Interestingly, in PMA-treated proapoptotic D2 cells, two nuclear restricted pre-mRNA binding proteins, heterogeneous nuclear

ribonucleoprotein C1 and C2, are translocated to the cytosolic compartment in a ROCK-dependent manner (56). Notably, analysis of PKC-regulated genes in LNCaP cells revealed a number of Rho-GEFs that become up-regulated in response to PMA, including ARHGEF2, ARHGEF10, and ARHGEF12, as well as Rho-GAPs that become down-regulated, such as ARHGAP11a and ARHGAP19.[4] The relative contributions of these Rho modulators in prostate cancer cells still need to be determined.

Our studies also implicate the cell cycle inhibitor p21^{Cip1} as a mediator of PMA-induced apoptosis in prostate cancer cells. It is well established that in many cell types, PMA stimulation leads to the induction of p21^{Cip1}, and this induction plays a central role in PMA-induced growth inhibition (4, 5). Previous studies from our laboratory in lung cancer cells showed that PKCδ controls p21^{Cip1} induction at a transcriptional level, whereas other PKCs are less important for controlling the expression of this cell cycle inhibitor (4). Early studies established that p21^{Cip1} induction and retinoblastoma dephosphorylation preceded PMA-induced apoptosis in LNCaP cells (10). We found that impeding p21^{Cip1} induction using RNAi attenuates cell death in response to the phorbol ester. Recently, studies in prostate and colon cancer cell lines showed that p21^{Cip1} up-regulation is essential for TRAIL sensitization by proteasome inhibitors (57) and HDAC inhibitors (58), highlighting the relevance of this cell cycle inhibitor in sensitizing for cell death induced by cytokines, as suggested by our studies. We also determined that p21^{Cip1} up-regulation by PMA is ROCK-dependent. The regulation of p21^{Cip1} by Rho family members is controversial, since Rho was found to either suppress or induce the expression of cell cycle inhibitors, depending on the cell type (59–61). In contrast to our studies in prostate cancer cells, PMA-treated D2 erythromyeloblasts, the proapoptotic population has impaired p21^{Cip1} up-regulation resulting from ROCK activation, suggesting major cell type differences in the control of the pathway. JNK has been also linked to p21^{Cip1} expression (62). However, although in LNCaP cells JNK activation is ROCK-dependent, a JNK inhibitor does not abrogate p21^{Cip1} induction, suggesting the involvement of parallel pathway(s). Although p21^{Cip1} up-regulation in some cell types is dependent upon the activation of the MEK-ERK pathway (60), Y-27632 did not affect ERK phosphorylation by PMA in LNCaP cells (data not shown), suggesting that in our model, ROCK regulation of p21^{Cip1} is ERK-independent. Indeed, our previous studies showed that a MEK inhibitor enhances PMA-induced apoptosis (28). A p38 inhibitor also failed to impair p21^{Cip1} induction by PMA in LNCaP cells (data not shown). Although MAPK cascades exert transcriptional effects via Sp1 transcription factors, deletion of Sp1 sites in the human p21^{Cip1} promoter abrogates the induction by PMA. As PMA exerts pleiotropic effects on signaling cascades, it is conceivable that MAPK-independent pathways modulate p21^{Cip1} transcriptional activation, such as direct phosphorylation of Sp1 by protein kinase G, cyclin-dependent kinases, or other kinases (46, 63, 64).

In summary, our studies showed that RhoA/ROCK and the cytoskeleton are implicated in PMA-induced apoptosis in prostate cancer cells. A key role for the cell cycle inhibitor p21^{Cip1} has also been identified in the context of Rho signaling. A model summarizing our findings is depicted in Fig. 6*B*. A considerable amount of effort has been devoted to developing PKC modulators with anti-cancer therapeutic value, although selective agonists for PKCδ as antimitogenic/proapoptotic agents have yet to be developed. The elucidation of the PKCδ downstream effectors is highly relevant to understanding the basis of cell growth inhibition and apoptosis mediated by this kinase. The identification of Rho/ROCK as a mediator of PKCδ-driven apoptosis may provide a novel platform for the design of PKC modulators for cancer treatment.

REFERENCES

1. Newton, A. C. (2001) *Chem. Rev.* **101,** 2353–2364
2. Griner, E. M., and Kazanietz, M. G. (2007) *Nat. Rev. Cancer* **7,** 281–294
3. Barry, O. P., and Kazanietz, M. G. (2001) *Curr. Pharm. Des.* **7,** 1725–1744
4. Nakagawa, M., Oliva, J. L., Kothapalli, D., Fournier, A., Assoian, R. K., and Kazanietz, M. G. (2005) *J. Biol. Chem.* **280,** 33926–33934
5. Black, J. D. (2000) *Front. Biosci.* **5,** D406–D423
6. Afrasiabi, E., Ahlgren, J., Bergelin, N., and Törnquist, K. (2008) *Mol. Cell. Endocrinol.* **292,** 26–35
7. Fujii, T., García-Bermejo, M. L., Bernabó, J. L., Caamaño, J., Ohba, M., Kuroki, T., Li, L., Yuspa, S. H., and Kazanietz, M. G. (2000) *J. Biol. Chem.* **275,** 7574–7582
8. Yin, L., Bennani-Baiti, N., and Powell, C. T. (2005) *J. Biol. Chem.* **280,** 5533–5541
9. Truman, J. P., Gueven, N., Lavin, M., Leibel, S., Kolesnick, R., Fuks, Z., and Haimovitz-Friedman, A. (2005) *J. Biol. Chem.* **280,** 23262–23272
10. Zhao, X., Gschwend, J. E., Powell, C. T., Foster, R. G., Day, K. C., and Day, M. L. (1997) *J. Biol. Chem.* **272,** 22751–22757
11. Gonzalez-Guerrico, A. M., and Kazanietz, M. G. (2005) *J. Biol. Chem.* **280,** 38982–38991
12. Xiao, L., Gonzalez-Guerrico, A., and Kazanietz, M. G. (2009) *Mol. Carcinog.* **48,** 187–195
13. Jaffe, A. B., and Hall, A. (2005) *Annu. Rev. Cell Dev. Biol.* **21,** 247–269
14. Etienne-Manneville, S., and Hall, A. (2002) *Nature* **420,** 629–635
15. Riento, K., and Ridley, A. J. (2003) *Nat. Rev. Mol. Cell Biol.* **4,** 446–456
16. Shi, J., and Wei, L. (2007) *Arch. Immunol. Ther. Exp.* **55,** 61–75
17. Coleman, M. L., Sahai, E. A., Yeo, M., Bosch, M., Dewar, A., and Olson, M. F. (2001) *Nat. Cell Biol.* **3,** 339–345
18. Sebbagh, M., Renvoizé, C., Hamelin, J., Riché, N., Bertoglio, J., and Bréard, J. (2001) *Nat. Cell Biol.* **3,** 346–352
19. Lai, J. M., Hsieh, C. L., and Chang, Z. F. (2003) *J. Cell Sci.* **116,** 3491–3501
20. Del Re, D. P., Miyamoto, S., and Brown, J. H. (2007) *J. Biol. Chem.* **282,** 8069–8078
21. Pan, Q., Bao, L. W., Teknos, T. N., and Merajver, S. D. (2006) *Cancer Res.* **66,** 9379–9384
22. Chang, Y. C., Lee, H. H., Chen, Y. J., Bokoch, G. M., and Chang, Z. F. (2006) *Cell Death Differ.* **13,** 2023–2032
23. Mehta, D., Rahman, A., and Malik, A. B. (2001) *J. Biol. Chem.* **276,** 22614–22620
24. Slater, S. J., Seiz, J. L., Stagliano, B. A., and Stubbs, C. D. (2001) *Biochemistry* **40,** 4437–4445
25. De Siervi, A., Marinissen, M., Diggs, J., Wang, X. F., Pages, G., and Senderowicz, A. (2004) *Cancer Res.* **64,** 743–750
26. Ren, X. D., and Schwartz, M. A. (2000) *Methods Enzymol.* **325,** 264–272
27. Liu, P. Y., and Liao, J. K. (2008) *Methods Enzymol.* **439,** 181–189
28. Tanaka, Y., Gavrielides, M. V., Mitsuuchi, Y., Fujii, T., and Kazanietz, M. G. (2003) *J. Biol. Chem.* **278,** 33753–33762
29. Marinissen, M. J., Chiariello, M., Tanos, T., Bernard, O., Narumiya, S., and Gutkind, J. S. (2004) *Mol. Cell.* **14,** 29–41
30. Potin, S., Bertoglio, J., and Bréard, J. (2007) *FEBS Lett.* **581,** 118–124

---

[4] V. Von Burstin, M. C. Caino, and M. G. Kazanietz, unpublished observations.

31. Unterseher, F., Hefele, J. A., Giehl, K., De Robertis, E. M., Wedlich, D., and Schambony, A. (2004) *EMBO J.* **23,** 3259–3269

32. Schavinsky-Khrapunsky, Y., Huleihel, M., Aboud, M., and Torgeman, A. (2003) *Oncogene* **22,** 5315–5324

33. Park, J. W., Jang, M. A., Lee, Y. H., Passaniti, A., and Kwon, T. K. (2001) *Biochem. Biophys. Res. Commun.* **280,** 244–248

34. el-Deiry, W. S., Tokino, T., Velculescu, V. E., Levy, D. B., Parsons, R., Trent, J. M., Lin, D., Mercer, W. E., Kinzler, K. W., and Vogelstein, B. (1993) *Cell* **75,** 817–825

35. Gartel, A. L., and Tyner, A. L. (1999) *Exp. Cell Res.* **246,** 280–289

36. Pan, J., Singh, U. S., Takahashi, T., Oka, Y., Palm-Leis, A., Herbelin, B. S., and Baker, K. M. (2005) *J. Cell. Physiol.* **202,** 536–553

37. Meacci, E., Donati, C., Cencetti, F., Romiti, E., and Bruni, P. (2000) *FEBS Lett.* **482,** 97–101

38. Harrington, E. O., Shannon, C. J., Morin, N., Rowlett, H., Murphy, C., and Lu, Q. (2005) *Exp. Cell Res.* **308,** 407–421

39. García-Mata, R., and Burridge, K. (2007) *Trends Cell Biol.* **17,** 36–43

40. Ohtsu, H., Mifune, M., Frank, G. D., Saito, S., Inagami, T., Kim-Mitsuyama, S., Takuwa, Y., Sasaki, T., Rothstein, J. D., Suzuki, H., Nakashima, H., Woolfolk, E. A., Motley, E. D., and Eguchi, S. (2005) *Arterioscler. Thromb. Vasc. Biol.* **25,** 1831–1836

41. Slater, S. J., Cook, A. C., Seiz, J. L., Malinowski, S. A., Stagliano, B. A., and Stubbs, C. D. (2003) *Biochemistry* **42,** 12105–12114

42. Lyons, L. S., and Burnstein, K. L. (2006) *Mol. Endocrinol.* **20,** 1061–1072

43. Wang, Q., Liu, M., Kozasa, T., Rothstein, J. D., Sternweis, P. C., and Neubig, R. R. (2004) *J. Biol. Chem.* **279,** 28831–28834

44. Chang, Z. F., and Lee, H. H. (2006) *J. Biomed. Sci.* **13,** 173–180

45. Papadopoulou, N., Charalampopoulos, I., Alevizopoulos, K., Gravanis, A., and Stournaras, C. (2008) *Exp. Cell Res.* **314,** 3162–3174

46. Chu, S., and Ferro, T. J. (2005) *Gene* **348,** 1–11

47. Mills, J. C., Stone, N. L., Erhardt, J., and Pittman, R. N. (1998) *J. Cell Biol.* **140,** 627–636

48. Orlando, K. A., and Pittman, R. N. (2006) *Exp. Cell Res.* **312,** 3298–3311

49. Cohen, O., Inbal, B., Kissil, J. L., Raveh, T., Berissi, H., Spivak-Kroizaman, T., Feinstein, E., and Kimchi, A. (1999) *J. Cell Biol.* **146,** 141–148

50. Jin, Y., Atkinson, S. J., Marrs, J. A., and Gallagher, P. J. (2001) *J. Biol. Chem.* **276,** 30342–30349

51. Chaigne-Delalande, B., Moreau, J. F., and Legembre, P. (2008) *Arch. Immunol. Ther. Exp.* **56,** 9–14

52. Yanazume, T., Hasegawa, K., Wada, H., Morimoto, T., Abe, M., Kawamura, T., and Sasayama, S. (2002) *J. Biol. Chem.* **277,** 8618–8625

53. Marinissen, M. J., Chiariello, M., and Gutkind, J. S. (2001) *Genes Dev.* **15,** 535–553

54. Berenjeno, I. M., and Bustelo, X. R. (2008) *Clin. Transl. Oncol.* **10,** 726–738

55. Miralles, F., and Visa, N. (2006) *Curr. Opin. Cell Biol.* **18,** 261–266

56. Lee, H. H., Chien, C. L., Liao, H. K., Chen, Y. J., and Chang, Z. F. (2004) *J. Cell Sci.* **117,** 5579–5589

57. Lashinger, L. M., Zhu, K., Williams, S. A., Shrader, M., Dinney, C. P., and McConkey, D. J. (2005) *Cancer Res.* **65,** 4902–4908

58. Nawrocki, S. T., Carew, J. S., Douglas, L., Cleveland, J. L., Humphreys, R., and Houghton, J. A. (2007) *Cancer Res.* **67,** 6987–6994

59. Croft, D. R., and Olson, M. F. (2006) *Mol. Cell. Biol.* **26,** 4612–4627

60. Lai, J. M., Wu, S., Huang, D. Y., and Chang, Z. F. (2002) *Mol. Cell. Biol.* **22,** 7581–7592

61. Coleman, M. L., Densham, R. M., Croft, D. R., and Olson, M. F. (2006) *Oncogene* **25,** 2708–2716

62. Kim, C. G., Choi, B. H., Son, S. W., Yi, S. J., Shin, S. Y., and Lee, Y. H. (2007) *Cell. Signal.* **19,** 1290–1300

63. Cen, B., Deguchi, A., and Weinstein, I. B. (2008) *Cancer Res.* **68,** 5355–5362

64. Fojas de Borja, P., Collins, N. K., Du, P., Azizkhan-Clifford, J., and Mudryj, M. (2001) *EMBO J.* **20,** 5737–5747